Assessing the Impact of Variations in Atmospheric Water Vapour Content over Nigeria from GNSS Measurements

[1,3] Olalekan Adekunle Isioye, [1]Ludwig Combrinck, [2]Joel Ondego Botai , [3]Mefe Moses

[1] Department of Geography, Geoinformatics and Meteorology, University of Pretoria, South Africa, olalekanisioye@gmail.com
[2]South African Weather Service, 442 Rigel Avenue South, Erasmusrand, Pretoria 0001, South Africa
[3]Department of Geomatics, Ahmadu Bello University, Zaria – Nigeria

Abstract

This study analyses the meteorological impact of the variability of precipitable water vapour (PWV) retrieved from ground-based global navigation satellite system (GNSS) stations over Nigeria from 2013 to 2014; these measurements represent the foremost probe of GNSS PWV distribution and variability over Nigeria. In this study, GNSS PWV daily estimates were grouped into monthly and seasonal averages; the variations in the monthly and seasonal estimates of GNSS PWV were characterized and correlated with different weather events that are regarded as good climate change indicators. The results revealed that the spatiotemporal changes in PWV content are largely subjugated by the effects of latitude, topographical features, the seasons and the continental air masses. Our study shows that there is a very strong seasonal interplay among the GNSS PWV, relative humidity, rainfall and cloud estimates. In addition, GNSS PWV and total electron content (TEC) estimates show an opposite relationship; the semi-diurnal relationship between GNSS PWV and TEC is stronger than the seasonal relationship. The seasonal relation among GNSS PWV, temperature and wind speed appears weak, while very strong interplay exists among the GNSS PWV, sun spot number and total solar radiation estimates. Our results confirm that GNSS PWV is a good pointer for weather forecasting/monitoring and fit for climate monitoring if available on a longer time scale. Finally, we recommend the densification of the GNSS network in Nigeria, as this will enable 3D profiling of PWV, thereby providing more information on GNSS PWV time series, which is needed for long-term climatology.

Keywords: *Global Navigation Satellite System (GNSS), Rainfall events, Solar events, Precipitable water vapour (PWV), and Climate indicators*

1. Introduction and Background

Atmospheric water vapour is one of the crucial factors in the investigation of global climate systems, especially over low latitudes where water vapour exhibits significant seasonal changes (Musa et al. 2011). Lack of detailed understanding of the global distribution of atmospheric water vapour in space and time is the major limiting factor in the precise forecast of weather and climate

using numerical models. Thus, more all-inclusive data sets are required to comprehend climate and weather patterns fully.

In recent years, it has been shown that ground-based global navigation satellite system (GNSS) receivers provide valuable information on precipitable water vapour (PWV) in the troposphere (e.g. Jin and Luo 2009; Liang et al. 2015). This is achieved by calculating the approximate time changing zenith wet delay (ZWD), which is reclaimed by stochastic filtering of raw GNSS observations (e.g. Bevis et al. 1992; 1994). GNSS has huge advantages over other systems for observing PWV, since it is a system that works in all weather conditions, with continuous unattended operation, good time resolution and a continual increase in the number of stations in many regions of the world.

Several feasibility studies have demonstrated the usefulness of the GNSS meteorology method; extensive experiments have so far shown that PWV can be obtained with an accuracy of better than 2 mm (or at the 5% level) from global positioning system (GPS)/GNSS observations (Karabatic et al. 2011). Near-real-time (NRT) applications of zenith tropospheric delay (ZTD) and PWV have been investigated (see Gendt et al. 2004; Lu et al. 2015) and are shown to provide highly accurate results in NRT for forecasting models. Also, several studies have concluded that GNSS provides information that yields better prediction of extreme weather conditions, such as thunderstorms (e.g. Jerrett and Nash 2001), lightning (e.g. Mazany et al. 2002, and references in it), typhoons (e.g. Song and Grejner-Brzezinska 2009), night-time fog or intense precipitation (e.g. Liang et al. 2015; Benevides et al. 2015) and flooding (e.g. Katsougiannopoulos et al. 2015; Sharifi et al. 2015, and references therein). PWV derived GNSS observations have also been correlated with total electron content (TEC) from the same observation system to study the response of PWV to solar activities (see, Suparta et al. 2008; Suparta and Fraser 2014).

Over the past few years, various government agencies around the world have launched projects to establish ground-based GPS/GNSS meteorological networks for operational meteorology and many meteorological institutes all over the world have successfully assimilated ZTD and/or PWV data into numerical weather prediction (NWP) models. For example, the Forecasting System Laboratory of the National Oceanic and Atmospheric Administration in the USA has established a GPS precipitable water vapour (GPS-PWV) network, which currently produces PWV solutions on an hourly basis for operational weather-forecasting purposes (see Gutman et al. 2004 and references in it). In Japan, the Geospatial Information Authority of Japan is operating a nationwide GNSS network, called the GNSS Earth Observation Network System (GEONET), which has a mean horizontal spacing of approximately 20 km. The Meteorological Research Institute and the Japanese Meteorological Agency (see Koizumi and Sato 2004) have extensively tested the use of GEONET-derived water vapour data to support NWP models. In China, the China Meteorological Administration (CMA) has about 952 GNSS sites, which produce NRT water vapour for weather diagnoses and forecasting applications; PWV from CMA network has already been assimilated into the GRAPES_RAFS weather model (see Liang et al. 2015 and references in it). The Meteorological Office in the UK (Jerrett and Nash 2001), MeteoSwiss in Switzerland (Guerova et al. 2006), the German Weather Service (Gendt et al., 2004), the Instituto Nacional de Meteorologia together with the institute of

Space Studies of Catalonia in Spain (Cucurull et al. 2004) and many other agencies around the world have all assimilated GNSS atmospheric products into different NWP models for operational use. The situation in Africa appears quite different; there are no records of GNSS products being assimilated into NWP models by meteorological offices/agencies in the region.

Their application in climate research is in contrast to NRT applications of GNSS atmospheric products. For climate applications, GNSS products are not required in NRT; instead highly accurate GNSS products are of the utmost importance. The spatial and long-term trends in water vapour content from GNSS have been useful in many studies focussed on climate monitoring in different regions around the world (e.g. Jin et al. 2007; Nilsson and Elgered 2008; Jin and Luo 2009). A further illustration of GNSS atmospheric products in climate research is the assessment of climate models (e.g. Ning et al. 2013).

In Nigeria, just like many other African countries, the application of the GNSS meteorology techniques for operational weather nowcasting and climate research is still unexploited. The Nigerian GNSS Network (NIGNET) is a network GNSS of 14 stations operated by the national mapping agency of Nigeria (or Office of the Surveyor General of the Federation (OSGOF)) that became operational in 2010. Now, meteorological/climatic use of data from the NIGNET is still limited by the density of the network and the duration of available data from the NIGNET, which is considered relatively short compared to the time scale of observable changes due to climate change. Nevertheless, it still offers a unique, reliable, and consistent source of data, which can help in nowcasting/synoptic applications and understanding/monitoring changes in the climate over Nigeria. The goal of the present study is to show the potential of using the NIGNET as a novel and active tool for a variety of meteorological applications (i.e., monitoring of weather events and possibly climate monitoring when long-time records are available). To achieve this goal, attention is focussed on three major studies. Firstly, the monthly and seasonal variation/trends in GNSS PWV estimates are looked into to provide pioneering knowledge for weather studies in Nigeria from GNSS observations. Secondly, rainfall events (humidity, rainfall, amount of cloud and wind speed) are correlated with PWV estimates to demonstrate the potential of GNSS meteorology for weather monitoring further. Lastly, the relation between PWV and solar activity (i.e. temperature, sunspot number (SSN), radiation, and interaction between the upper atmosphere (ionosphere) and the lower atmosphere (troposphere) as explained by TEC and PWV) were investigated to explain interactions between terrestrial weather/climate changes and solar activity.

In this paper, the different data sets used in the study and procedures for estimation of TEC and PWV are presented in Section 2. In Section 3, the variability of GNSS-PWV over Nigeria is outlined. Section 4 investigates the relationship between GNSS-PWV and rainfall events over Nigeria. In Section 5, the relationship between GNSS-PWV and solar events over Nigeria is investigated. The summing up and concluding remarks are given in the final part.

2. Data and Methodology

Daily GNSS observation data files in RINEX format with a 30-seconds sampling rate were collected from seven stations representing the different climatic zones in Nigeria for the period 2013-2014 via file transfer protocol (ftp) from the NIGNET server (http://server.nignet.net/). The GNSS stations were carefully selected based on their proximity to automatic (synoptic) weather observing stations (AWOS), as shown in Figure 1. Data from the AWOS were obtained from the Nigerian Meteorological agency (NIMET). The GAMIT/GLOBK software (Herring et al. 2006) was used to estimate the ZTD. It employs a forced batch least squares inversion process. The GAMIT/GLOBK software parameterises the ZTD as a stochastic deviation of the uncomplicated representation of the Saastamoinen hydrostatic delay model (see Saastamoinen 1972) with a Gauss–Markov power density of $2cm/hour^{1/2}$.
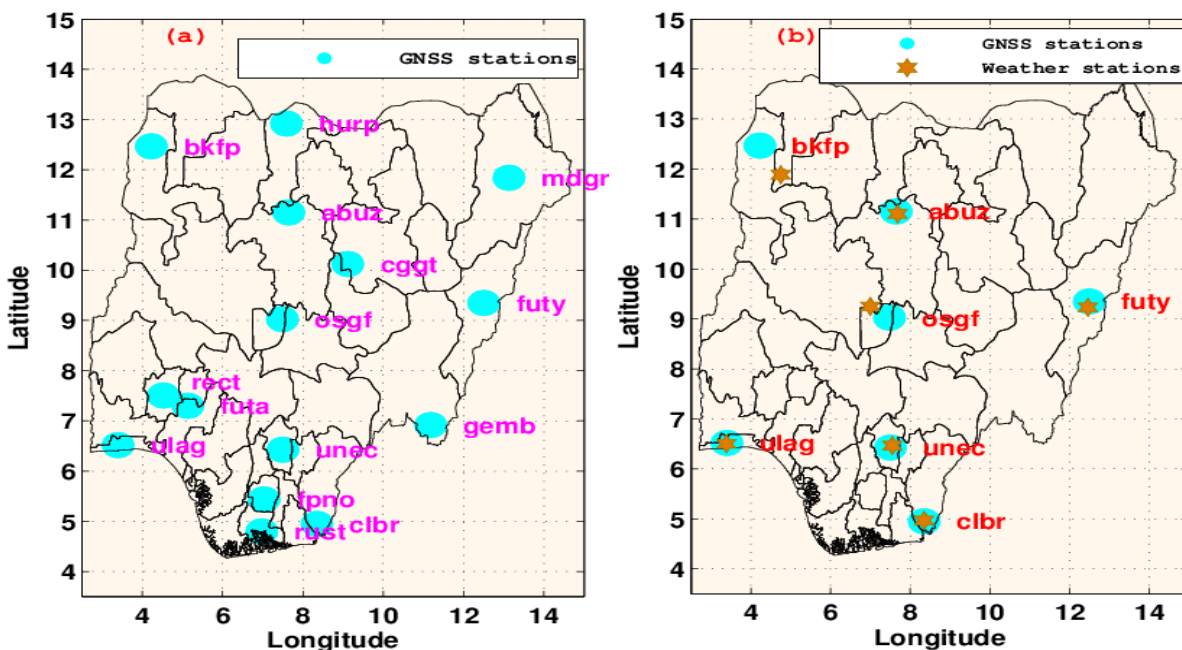

Figure 1: Location of GNSS sites in Nigeria (a) depicts all the stations in the new NIGNET under the management of the OSGOF (b) shows the seven chosen GNSS stations and matching AWOS sites at which PWV was estimated for this study

The ZTD at each GNSS station was estimated two-hourly and daily within a 24-hour window session. The International GNSS Service (IGS) final orbits (SP3) and IGS final Earth rotation parameter (ERP) products were used. Satellite elevation cut-off was set to 10° during the data processing. Station coordinates were heavily constrained to their ITRF 2008 values (Altamimi et al. 2011). Solid earth tide based on the IERS03 and FES2004 models were used for solid earth tide and ocean tide loading corrections, respectively. The constraint used for zenith delay was 0.2 m, as it is recommended to set it loosely enough to encompass any error in wet delay (Herring et al. 2006). Satellite antenna phase centre offset and phase centre variation is based on AZEL for IGS absolute ANTEX files (Gendt and Schmid 2005). The a priori tropospheric model used is the Saastamoinen model (1972) based on meteorological sources from the Global Pressure and Temperature (GPT) model. The Vienna Mapping Function (Boehm et al. 2006) was used to calculate the zenith delay. To

retrieve PWV estimates from GNSS-derived ZTDs, station temperature and pressure values are fundamental to separate the ZTD into its wet and dry components. Thus, surface temperature and pressure data from nearby AWOS (see Figure 1) were transferred to the GNSS sites employing the technique demonstrated by Musa et al. (2011). The resultant ZWD component was transformed to PWV using the following relation (Bevis et al. 1992; Isioye et al. 2015):

$$PWV = \frac{\left[ZTD_{GNSS} - ZHD\right]}{10^{-6} R_w \rho_w \left[k_2' + \frac{k_3}{T_m} \right]} = \Pi \left[ZTD_{GNSS} - ZHD\right] = \Pi \cdot ZWD \ . \tag{1}$$

In Equation (1), $\rho_w = 1025 \ kg/m^3$ is the density of liquid water, $R_w = 461.525 \pm 0.003 \left(Jkg^{-1}K^{-1}\right)$ is the specific gas constant for water vapour. k_2' and k_3 are refraction constants, where $k_2' = 22.1 \pm 2.2 \ K \ hPa^{-1}$ and $k_3 = 373900 \pm 0.012 \ K^2 hPa^{-1}$ and T_m is the mean water vapour temperature of the atmosphere measured in Kelvin (K). The Nigeria Weighted Mean Temperature Equation (NWMTE) is, according to Isioye et al. (2016), given as:

$$T_m = 0.5245 T_s + 132.12 \ . \tag{2}$$

In Equation (2), T_s is the surface temperature at the individual GNSS sites in Kelvin. The T_m and T_s relationship and associated parameters in Equation (2) are based on the refinement of the Bevis formula (see Bevis et al., 1994), since the relation is geographic location dependent. Thus, substituting the value of the constants and T_m into Equation (1), we derived a simplified expression for PWV as follows:

$$PWV = ZWD.\left[9.80392 - \frac{16917.64}{0.053499 T_s + 1739.07624} \right] \ . \tag{3}$$

Equation (3) is suggested to users as a handy formula to estimate PWV (in mm) in Nigeria using $T_s(K)$ and ZWD (mm) as inputs.

The TEC processing was carried out using the available GNSS observation data, satellite navigation data and the differential code bias (DCB) files by means of the free GPS-TEC analysis v2.2 software (http://seemala.blogspot.com), developed by Gopi Seemata at Boston College, USA. In this study, DCB for all satellites is obtained from the Centre for Orbit Determination in Europe, University of Bern, Switzerland (ftp://ftp.unibe.ch/~ aiub/CODE) and the software estimates DCBs for the ground GNSS station. The TEC is a pointer of ionospheric inconsistency that is derived from the adapted GNSS signals through free electrons. Diverse epochs of ionospheric interactions can be considered by identifying and analysing the temporal variations in TEC. TEC is defined as the total number of electrons integrated along the path from the satellite to the receiver and can be written as (Zoundi et al. 2012):

$$TEC = \int_{Receiver}^{Satellite} N_e dh \ . \tag{4}$$

In Equation (4), N_e *is the* electron density down the ray paths from the satellite in space to the ground receiver. TEC is measured in units of 10^{16} electrons meter per square area, where

10^{16} *electron* / m^2 is equal to 1 TEC unit. As the TEC between the satellite and user receiver relies on the satellite elevation angle, the measure is the slant TEC. For practical applications the vertical TEC, which is free of elevation of the ray path, is often used and acquired from the slant TEC using the thin shell or single layer and mapping function of the simple layer model as follows (Norsuzila et al. 2009):

$$Vertical\ TEC = Slant\ TEC \times \cos\left[\sin^{-1}\left(\frac{R_e\cos\theta}{R_e + h_{max}}\right)\right] . \qquad [5]$$

In Equation (5), θ is the elevation angle at the ground station, $R_e = 6378km$ is the radius of the earth, and h_{max} is the maximum electron density height assumed in the model with a typical value of 350 km.

Quality-controlled monthly rainfall, relative humidity, wind speed and temperature (maximum and minimum) data over AWOS near GNSS sites in Nigeria were collected from the records of the NIMET, for a period of two years (2013-2014). Similarly, average monthly normal radiation and daylight cloud amount at the respective GNSS sites were obtained from the atmospheric science data centre of NASA (see https://eosweb.larc.nasa.gov/cgi-bin/sse/grid.cgi). Monthly predicted SSN for the period under investigation was obtained from the Solar Influence Data Analysis Centre, Royal Observatory of Belgium, Brussels (see http://www.sidc.be/SILSO/).

Similarly, GNSS PWV values were averaged into monthly values to correlate them with the other weather events (TEC, temperature, SSN, radiation, rainfall, humidity, wind speed and daylight cloud amount) and to understand the distribution of PWV by month. To investigate seasonal variations, data were divided into four seasonal groups. The months of March, April and May (MAM) are the hottest in the north, with few records of rain in the southern part of Nigeria. The peak of the wet season in all parts of Nigeria is in the months of June, July and August (JJA). The months of September, October and November (SON) signify the end of the wet season in the north, while in the south, it is a period often characterised by scanty rains and severe thunderstorms. The months of December, January and February (DJF) are dry in the north, with very low temperature, because of the Harmattan, while the south is dry and humid.

3. Variability of GNSS-PWV over Nigeria

Figure 2 shows the monthly variation of PWV for the duration of our limited years of study (from 2013-2014) at seven GNSS station locations representing the different climate zones in Nigeria. The Nigerian climate is categorised largely by interaction between the trade winds and also by the ecological zones (which change from tropical rainforest along the coast to semi-arid zones in the northern outer reaches). The lowest monthly PWV values at all the stations, as shown in Figure 2, were recorded in the months of December and January, with the northern stations (ABUZ, BKFP, FUTY, and OSGF) having lower PWV values than other stations (CLBR, ULAG and UNEC) in the southern part of Nigeria. The PWV values show an increasing trend from February until it reaches its maximum in July and August, then decreases toward December and January at all the stations. Again,

during the months with peak PWV values, stations in the southern part still have higher values of PWV compared to their counterparts in the north. From the foregoing it is obvious that the PWV values decrease from the south to the north of Nigeria or when moving from the stations in the coastal zones to the semi-arid zones. This pattern in the variability of PWV from the south to north may be attributed to the latitudinal dependence of PWV and/or the influence of the ocean on shorefronts. The stations (CLBR and ULAG) are located on the shorefront of the Atlantic Ocean around the coastal cities of Calabar and Lagos respectively. The PWV values at these GNSS stations when compared to the other stations are highest for all the months of the year. The high PWV values at CLBR and ULAG could in addition be attributed to the low elevation of the stations, which are at 57.13 m and 44.56 m respectively, compared to FUTY, BKFP, UNEC, OSGF and ABUZ at 247.39 m, 250 m, 254.39 m, 532.64 m, and 705.05 m respectively. There is a repetition of this trend at ABUZ; the monthly PWV value at ABUZ is lower than those of other northern stations, which are at higher latitude (i.e. BKFP) than ABUZ. Notably ABUZ has the highest station elevation among the GNSS stations and correspondingly the lowest PWV values for all the months. This is an indication that station elevation plays an important role in PWV estimates, as well the station latitude.
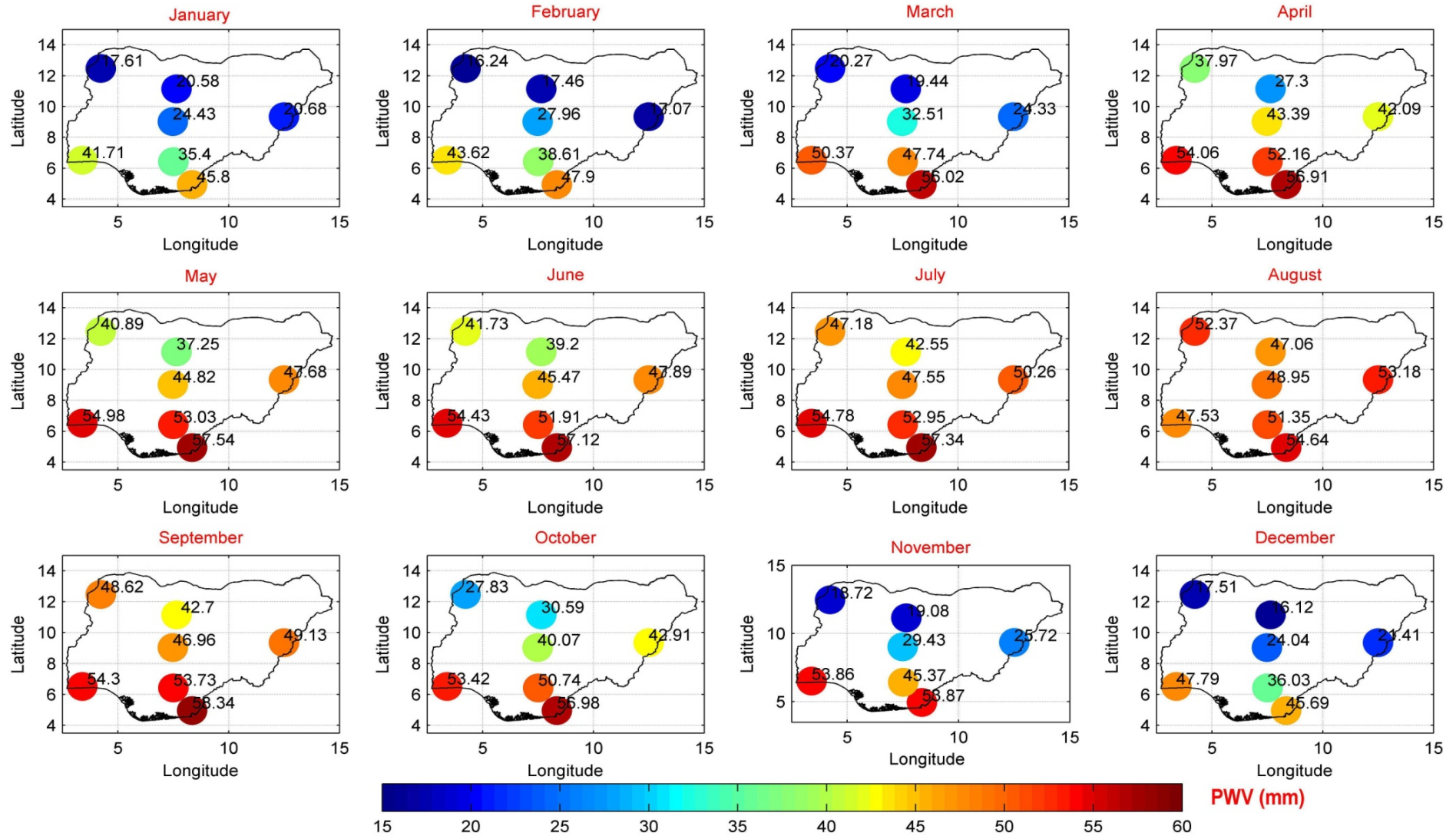
Figure 2: Monthly mean GNSS PWV (mm) for seven stations in different climatic regions of Nigeria from 2103 to 2014

Figure 3 presents the PWV values for the four seasons. According to Figure 3 the seasonal PWV confirms an apparent variation, with lower values in the dry season (DJF and MAM) and higher values in the wet season (JJA, SON), which reflects that in the wet (rainy) season, because of the strong moisture field (high water vapour pressure) the PWV magnitude is higher. PWV values at all the stations exhibit a recognised seasonal signal, which can be explained by a cosine function, as the increase to the maximum in the JJA season, which is the peak of the rainy season in both the north and south of Nigeria, and a decrease to the minimum in the months of DJF, the dry season in the south and the Harmattan in the north of Nigeria. There is little rain in the months of MAM and SON in the north and the temperature is high, while the south is not as dry as the north, thus the climate in the south is very humid and tends to keep the PWV values very high. PWVs vary spatially mainly according to altitude, though there is slight variation along both latitude and longitude over Nigeria. For instance, the magnitude of PWV is greater at all seasons along the shorefront of the Atlantic Ocean at CLBR and ULAG stations, which are in the lowlands.
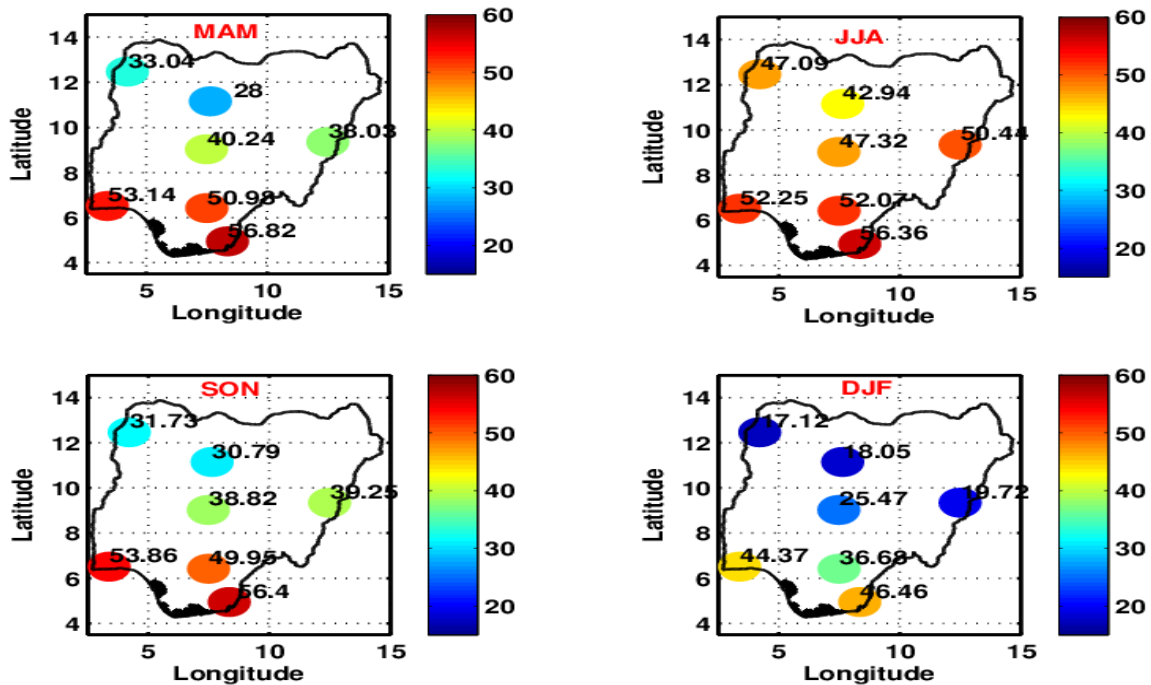

Figure 3: Seasonal mean GNSS PWV (mm) for MAM, JJA, SON, and DJF from 2013 to 2014

The seasonal range (i.e. difference between maximum and minimum seasonal values) of PWV at the different GNSS stations is 24.88 mm, 10.36 mm, 30.72 mm, 9.49 mm, 15.39 mm, 21.85 mm and 29.97 mm for ABUZ, CLBR, FUTY, ULAG, UNEC, OSGF, and BKFP, respectively. It is obvious that the range in PWV at most of the stations increases with latitude (i.e., movement from south to north). A sharp increase in the range values is seen at the location of GNSS stations (ABUZ, FUTY, OSGF, and BKFP) in the northern part of Nigeria. This is expected because of the extreme cold and hot weather during the dry season in the northern part of Nigeria, which often results in great variations in surface temperature.

The average annual PWV at ABUZ, CLBR, FUTY, ULAG, UNEC, OSGF, BKFP is 29.94 mm, 54.01 mm, 36.86 mm, 50. 90 mm, 47.42 mm, 37.96 mm and 32.25 mm, respectively. Again, the

lowest mean annual average value of PWV was recorded at ABUZ and the highest recorded at the lowland (and coastal) stations of CLBR and ULAG. Clearly, the PWV depends on the altitude and latitude. Figures 4 and 5 show the scatter plots of annual PWV values with the latitude and elevation of the corresponding GNSS stations, respectively. Both plots had negative slopes as an indication of an inverse relation between dependent and independent variables. A stronger coefficient of determination (goodness of fit) was found between PWV and station latitude $(R^2 = 0.9648)$, compared to the station elevation $(R^2 = 0.7916)$. This result is indicative of the latitudinal dependence of PWV. The climate of Nigeria is also known to vary from the south to the north (i.e. latitudinally), and this shows that GNSS PWV has good potential for climate studies and monitoring.
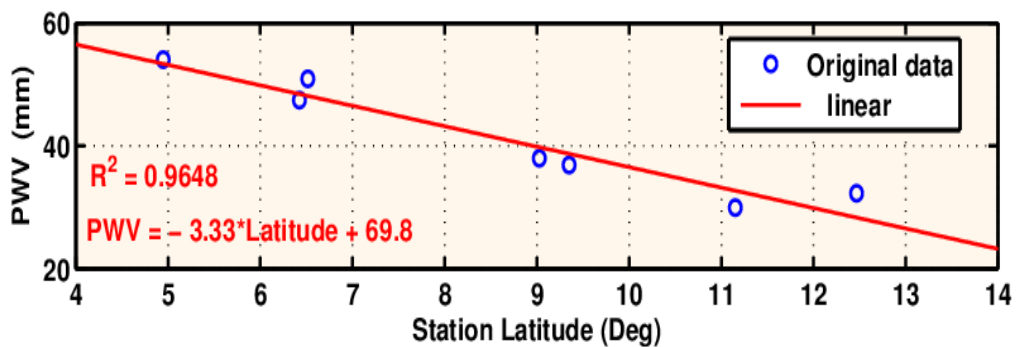

Figure 4: A scatter plot of the average PWV values at the different GNSS stations against the corresponding latitude of the GNSS station
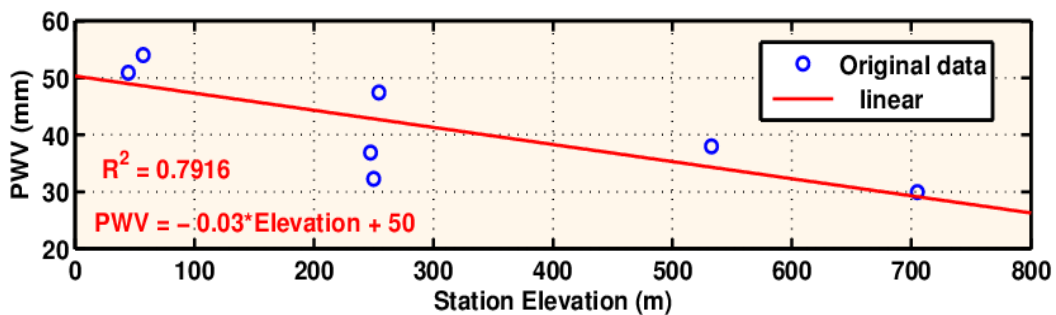

Figure 5: A scatter plot of the average PWV values at the different GNSS stations against the corresponding height of the GNSS station

In furthering earlier studies on the spatial dependence and temporal characteristics of GNSS-derived ZTD estimates in Nigeria as reported by Isioye et al. (2017), it will be of great importance to determine the interrelationship between GNSS PWV and GNSS ZTD. From equation (1), one can see the relationship between PWV and ZWD after separation of the dry and wet components of the ZTD. The value of Π typically varies from about 0.16 to 0.17 across the different seasons in Nigeria; as shown in Table 1, Π contributes more to the absolute derivation of PWV and largely depends on the choice of the model of T_m and its ability to respond to varying weather conditions in the adapted geographic region. The importance of using locally adapted models of T_m rather than the global and Bevis models has been articulated in many publications (i.e., Song & Grejner-Brzezinska 2009). Also,

from Table 1, it is evident that the variation in ZHD is unaccounted for by PWV; it largely depends on the variation in atmospheric pressure at the GNSS stations.

Table 1: Average GNSS PWV and GNSS ZTD relationships over Nigeria from 2013 to 2014

Station	Π	Coefficient of determination $\left(R^2\right)$			Regression $PWV = a\left(ZWD\right)+b$	
		PWV-ZTD	PWV-ZHD	PWV-ZWD	Slope $\left(a\right)$	Intercept $\left(b\right)$
ABUZ	0.1647	0.9958	0.0041	0.9998	0.1639	0.1241
BKFP	0.1644	0.9945	0.0256	0.9998	0.1635	0.2458
CLBR	0.1643	0.9941	0.0825	0.9996	0.1635	0.2500
FUTY	0.1647	0.9978	0.0724	0.9999	0.1637	0.1830
OSGF	0.1645	0.9886	0.0392	0.9998	0.1636	0.1946
ULAG	0.1647	0.9895	0.0386	0.9995	0.1639	0.2353
UNEC	0.1644	0.9939	0.0473	0.9998	0.1636	0.2037

Owing to the small variations in T_m , it can be seen that the PWV is mainly responsible for the variation in ZWD, as presented in Table 1. The PWV and ZWD relationship is a perfect correlation, and it is logical to accept that PWV bears the same spatial and temporal characteristics with ZTD, since it is obviously the major driving force in the ZTD estimates.

The discussion on GNSS PWV can benefit from the study of Isioye et al. (2017), which was based on a time series of two-hourly GNSS ZTD from 2010–2014 at 14 NIGNET stations. The study applied three spatial statistical models to the ZTD estimates, namely the ordinary least squares, spatial error model and spatial lag model. Diagnostic tests for independence of error terms, homogeneity of variance, normality and spatial dependence were performed for each model. Assumptions of all three models were not completely satisfactory and revealed weak spatial dependence among the stations (i.e. spatial autocorrelation was not obtained). This was attributed to the density of stations in the network; the GNSS PWV as estimated from the NIGNET over the same period is likely to follow suit. The diurnal and intra-seasonal variations of ZTD were also studied with GNSS measurements using the Mann-Kendall Trend test, Fisher's Kappa and Bartlett's Kolmogorov-Smirnov statistics. These were used to test for white noise in the ZTD estimates. The KPSS and Dickey-Fuller tests were used to test the stationarity of the ZTD time series. Tidal oscillations were noticed and reported at the GNSS stations. These oscillations were determined to have diurnal and semi-diurnal components. The diurnal components as seen from the ZTD were reported as the principal source of the oscillations. These outcomes can perhaps be ascribed to temporal variations in atmospheric water vapour on a diurnal scale. In addition, the diurnal ZTD cycles exhibited significant seasonal dependence, with larger amplitudes in the rainy (wet) season and smaller ones in the Harmattan (dry) season; the ZTD seasonal cycles are well in agreement with those PWVs observed in this study.

From the foregoing, it is evident that knowledge of the spatiotemporal changes of water vapour concentration may be of key significance to weather forecasting and monitoring and in the long term for climate research. It is important also to see how water vapour relates with other constituents of the atmosphere or weather events. In the preceding sections of this paper, discussions are focussed

on the interaction between the variability of water vapour and other climate indices, which include rainfall events and solar activity.

4. Investigation of GNSS-PWV and Rainfall Events over Nigeria

The frequency and intensity of severe weather events are projected to increase in response to the effects of global warming and meteorological and hydrological hazards, such as sudden increases in river levels or floods, may be caused (see Atedhor et al. 2011). Torrential rainfall is becoming a serious problem in the urban areas of Nigeria because such events may develop suddenly making it difficult to issue timely warnings to the public. The accurate prediction of localised heavy rain on a horizontal scale of several kilometres is still a challenging task in current mesoscale numerical prediction models, partly because of the lack of a now-casting meteorological observation network with fine spatial resolution in many different regions of the world (Adams et al. 2011). Information on water vapour is a particularly important factor in improving the prediction of heavy rain. Note that weather radar can detect a cloud only after precipitation starts. It is necessary, therefore, to develop an observation system that can monitor the local in-homogeneities of water vapour distributions that could be associated with the formation of convective clouds before torrential rains occur. The rainfall process is influenced by numerous diverse micro- and mesoscale physical and dynamic circumstances (i.e. atmospheric steadiness, vertical velocity, humidity, cloud type, terrain) and many other circumstances, which include water vapour (Sharifi et al. 2015). Water vapour is an extremely changeable element of the atmosphere and its variability over Nigeria, based on observations from GNSS, has already been discussed in a previous section of this report. It is essential to the transport of energy in the atmosphere and in the development and circulation of weather (Pikridas 2014). It is also the basis of rainfall and its latent heat is a significant element in the dynamics of most weather events (Suparta et al. 2008). Thus, in this section, monthly mean values of GNSS PWV are correlated with rainfall, relative humidity, daylight cloud amount and wind speed information to demonstrate the applicability of variability of GNSS PWV in climate studies.

Figures 6, 7, 8, 9, and 10 show the monthly variations of PWV with rainfall, relative humidity, daylight cloud amount and wind speed for the study period, respectively. In Figure 6, the rainfall amount is seen to increase with monthly PWV estimates at all the stations. The variation in the rainfall between the driest and wettest month is higher at ABUZ and BKFP, which are in the north of the country. Similar variation is seen in PWV estimates at these stations, as already discussed in section 2 of this paper. The high amount of rainfall in the south, as observed at CLBR and ULAG, corresponds with the PWV values at these stations, which are also higher than those at ABUZ and BKFP. At station ABUZ, the highest amount of rainfall was recorded in August and was plotted against GNSS PWV for the same period, as shown in Figure 7; the PWV was estimated at two-hour intervals and the rainfall was recorded twice a day (i.e., from 06:00 -18:00 and 18:00 to 06:00). In Figure 7 conspicuous peaks are seen in the GNSS PWV estimates hours before rainfall. However, because of the resolution of the rainfall records, the actual hours of rain corresponding to the peaks could not be ascertained. Similarly, depressions can be seen in Figure 6 on days or intervals of no

rain. This results further show that variability in PWV estimates as observed by GNSS is closely related to rainfall and confirms the efficiency of the GNSS meteorology technique in storm prediction and possibly also in improving future forecasting models in Nigeria, as already demonstrated in many other countries/regions of the world (Song & Grejner-Brzezinska 2009; Katsougiannopoulos 2015).

As seen from Figure 8, humidity is higher at CLBR and ULAG than at the other GNSS stations in the north of Nigeria. This obviously indicates that the coastal regions in the south are more humid (i.e. have a high amount of moist air) and have more potential capacity for rainfall. PWV, as observed from GNSS, has shown good agreement and interplay with rainfall amount and quantity of moisture in the air as indicated by the relative humidity. The higher the PWV content of the atmosphere, the more latent energy is available for the generation of storms. High temperatures in the north could also be attributed to the low amount of relative humidity and corresponding low PWV values. Daylight cloud amount, as shown in Figure 9, provides information on the visible mass of condensed watery vapour floating in the atmosphere. The cloud amount is high in the south and gradually decreases to the north with a wider range (difference between maximum and minimum value) from south to north. The cloud amount as depicted in Figure 9 is obviously in line with the GNSS-PWV trend at all the locations under investigation. Wind speed at 50 m, as shown in Figure 10, does not show any striking trend of variation at the GNSS stations in the different locations/regions in Nigeria, though an inverse relation is visible between the GNSS PWV values and the wind speed at each station.
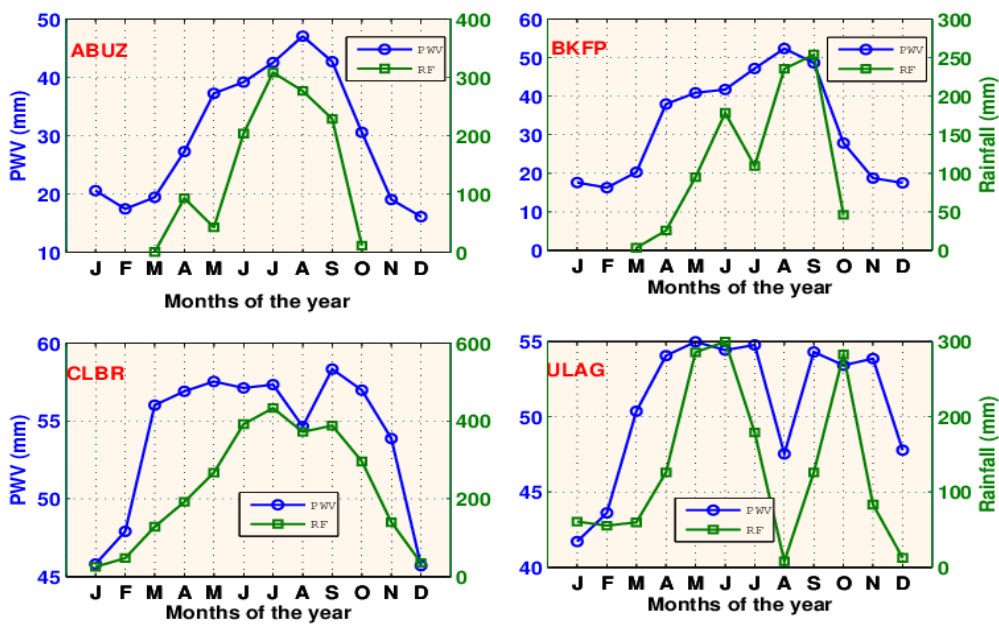

Figure 6: Monthly distribution of PWV (in blue) and rainfall amount (in green) at four GNSS stations (ABUZ, BKFP, CLBR, and ULAG) in Nigeria
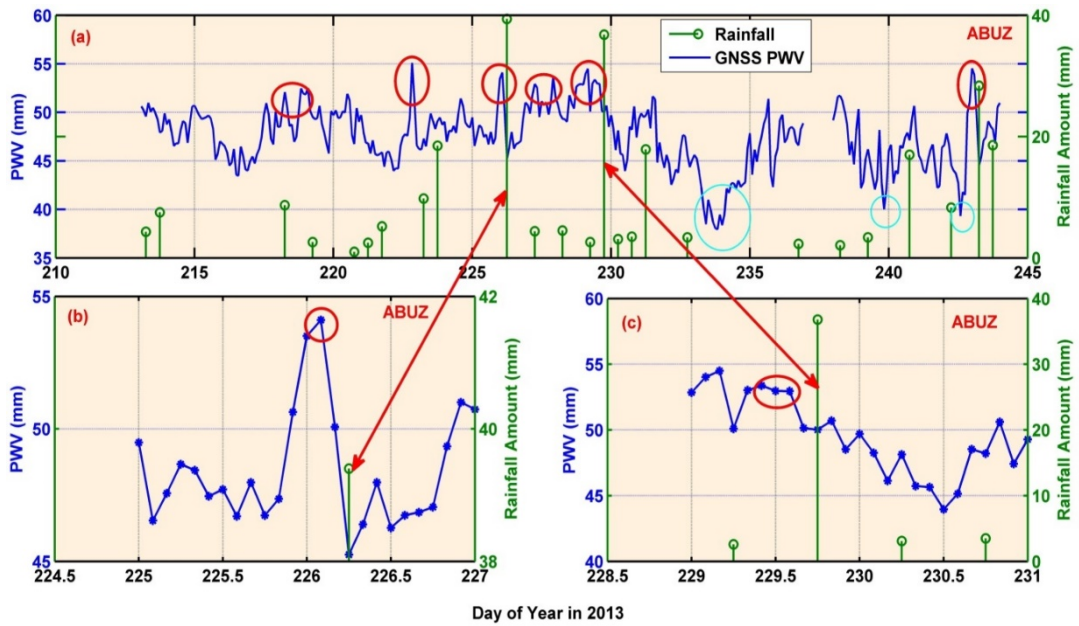
Figure 7: Distribution of PWV and rainfall in August 2013 at station ABUZ. The red circles indicate peaks in PWV estimates attributed to rainfall and cyan circles are tagged as depressions; (a) shows the distribution PWV alongside a 12-hourly record of rainfall, (b) is an exaggerated plot of the 14 August (DOY226) rainfall storm and (c) is an exaggerated plot of the 17 August (DOY 229) rainfall storm
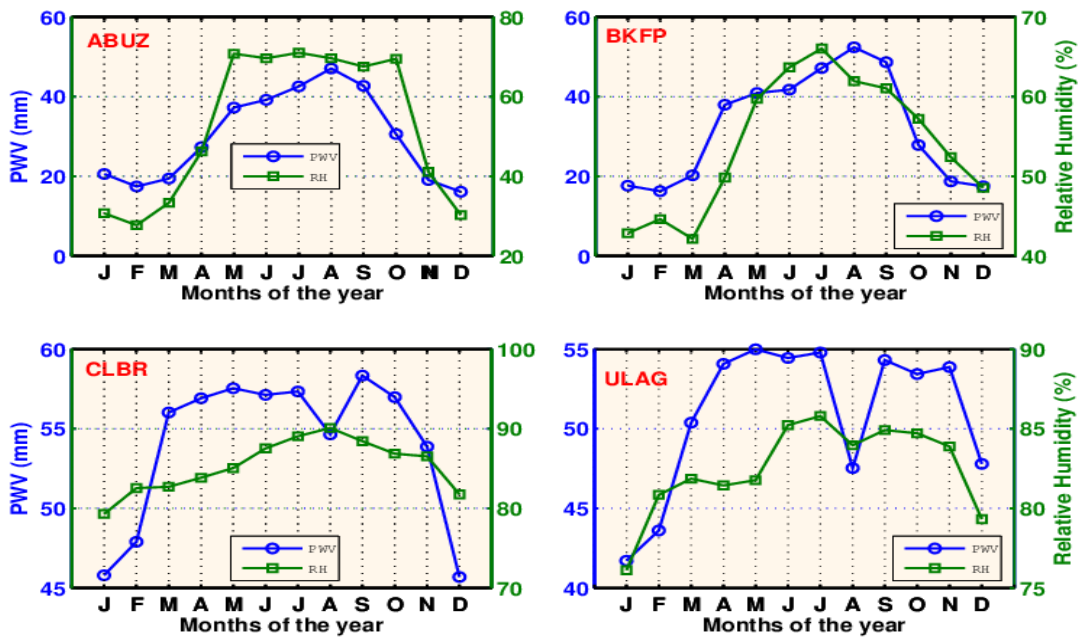

Figure 8: Monthly distribution of PWV (in blue) and relative humidity (in green) at four GNSS stations (ABUZ, BKFP, CLBR, and ULAG) in Nigeria
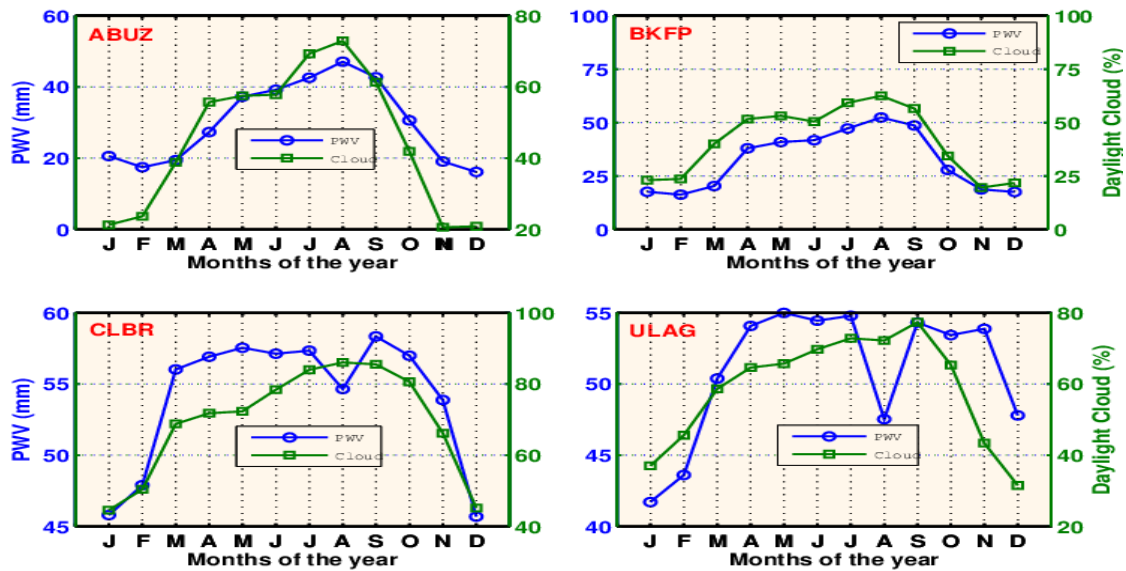
Figure 9: Monthly distribution of PWV (in blue) and daylight cloud amount (in green) at four GNSS stations (ABUZ, BKFP, CLBR, and ULAG) in Nigeria
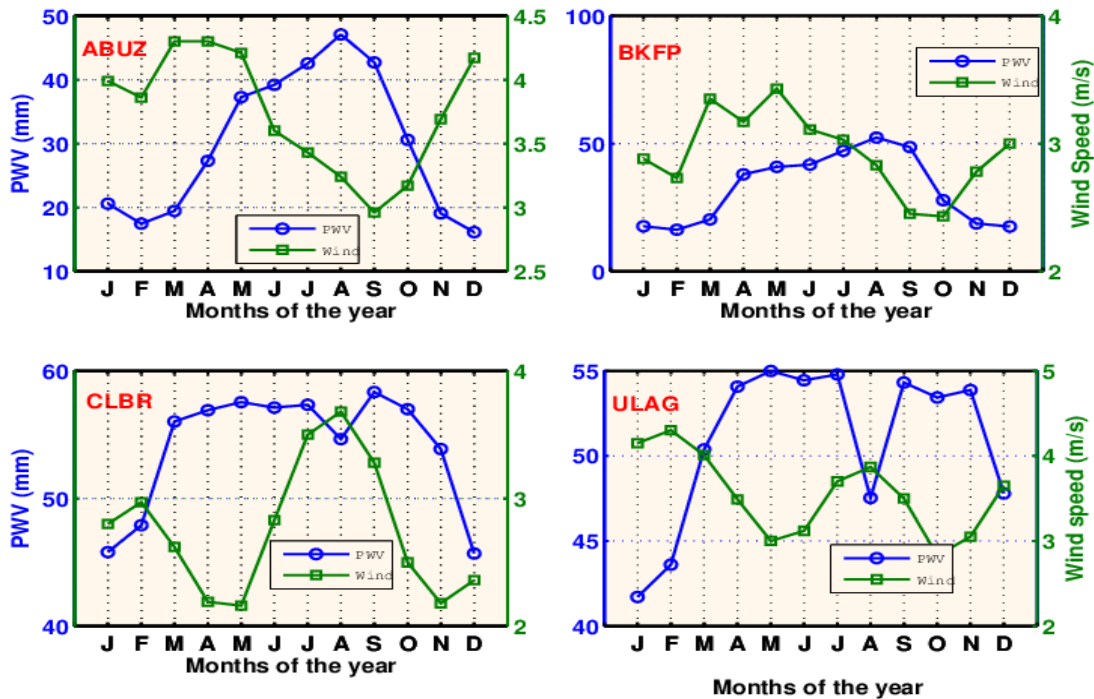

Figure 10: Monthly distribution of PWV (in blue) and wind speed (in green) at four GNSS stations (ABUZ, BKFP, CLBR, and ULAG) in Nigeria

To examine further how the climate indicators influence the study of weather/climate monitoring, it is ideal to describe the atmospheric system analytically and construct a general circulation model. However, this kind of model requires extensive data and massive numerical computations. Thus, we adopt a simple statistical approach of correlation analysis to further the interplay among the various climate indicators. The interplay among the different climate indicators as worked out from the Pearson's correlation coefficient test is presented in Table 2. GNSS PWV is seen to have a strong positive correlation with rainfall, humidity and the cloud amount at the different stations.

Interestingly, the rainfall, relative humidity and cloud amount also exhibit a positive correlation among themselves because of their direct dependence on each other at the individual stations. The wind speed exhibits the weakest correlation with the GNSS PWV at the different stations, except at ULAG with a strong negative correlation of -0.7897. In addition, there is no statistically significant correlation (at 95% confidence level) between wind speed and the other climate indicators at most of the stations, as shown by entries in red in Table (2).

Table 2: Pearson's correlation coefficient matrix for GNSS- PWV and the different rainfall events (rainfall, relative humidity (RH), wind, and daylight cloud amount) four GNSS locations in Nigeria.

Variables	GNSS- PWV	Rainfall	RH	Wind	Daylight cloud	GNSS- PWV	Rainfall	RH	Wind	Daylight cloud
			ABUZ					BKFP		
GNSS- PWV	1	0.8859	0.9269	-0.6356	0.9376	1	0.8848	0.8571	0.0235	0.9571
Rainfall		1	0.7146	-0.6044	0.8634		1	0.7916	-0.2195	0.7925
RH			1	-0.6310	0.8487			1	-0.1247	0.7314
Wind				1	-0.4264				1	0.2078
Daylight cloud					1					1
			CLBR					ULAG		
GNSS- PWV	1	0.8108	0.7273	0.0912	0.9172	1	0.6653	0.7544	-0.7897	0.6463
Rainfall		1	0.9119	0.5244	0.9378		1	0.6333	-0.5799	0.6879
RH			1	0.5152	0.9074			1	-0.5229	0.7713
Wind				1	0.4101				1	-0.3228
Daylight cloud					1					1

The coefficient of determination or goodness of fit $\left(R^2\right)$ between GNSS PWV and the other climate variables in the order of rainfall, humidity, wind speed and cloud amount at ABUZ is 0.7849, 0.8591, 0.4040, 0.8791, at BKFP it is 0.7829, 0.7349, 0.0006, 0.9161, at CLBR it is 0.6574, 0.5290, 0.0083, 0.8413, and at ULAG it is 0.4426, 0.5691, 0.6236, 0.4177, respectively. The R^2 values represented as percentages are shown in Figure 11; evidently, this result of the R^2 indicates that the variability in GNSS PWV can be adequately explained or predicted by similar variation in rainfall, humidity and cloud amount at the different GNSS locations under investigation. The predictability of GNSS PWV from wind speed observations as shown by the coefficient of determination still remains very weak at most of the stations or regions investigated. So, the relation as determined from the multivariate analysis between the different rain events (climate indicators) and GNSS PWV at the different regions can be given as follows:

$$\left.\begin{aligned}
GNSSPWV_{abuz} &= 13.33 + 0.24*Ra\text{infall} + 0.25*RH - 1.93*wind + 0.19*cloud \\
GNSSPWV_{bkfp} &= 7.361 - 0.02*Ra\text{infall} - 0.39*RH + 2.47*wind - 0.58*cloud \\
GNSSPWV_{clbr} &= 81.96 + 0.004*Ra\text{infall} - 0.58*RH - 2.7*wind + 0.40*cloud \\
GNSSPWV_{ulag} &= 31.49 + 0.005*Ra\text{infall} + 0.40*RH - 5.14*wind + 0.06*cloud
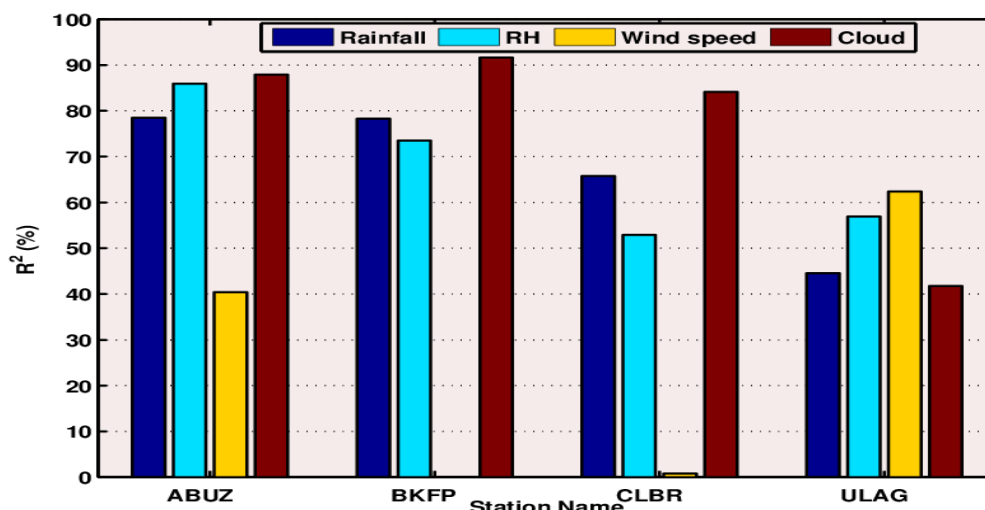\end{aligned}\right\} \quad . \quad (6)$$

Figure 11: The coefficient of determination (R^2 in %) between GNSS PWV and the other climate variables at four GNSS stations (ABUZ, BKFP, CLBR, and ULAG) in Nigeria

From the foregoing GNSS, PWV can seen as a constituent of the atmosphere with very highly variable characteristics constituting a major factor in climate and weather analysis, as demonstrated in this study. GNSS PWV and the other climate indicators can be used in forecasting different weather events and analysing the climate. However, climate analysis requires a much longer observation period.

5. Investigation of GNSS-PWV and Solar Events over Nigeria

In this section, we investigate the effect that the variability of solar activity has on weather parameters, namely the water vapour. A comprehensible correlation between water vapour and solar activity can elucidate some physical systems of how solar activities affect earthly weather. Many forms of solar activity, such as TEC, solar radiation bursts and solar wind, are known to be the basis for radiation enrichment and plasma movement, which are directly or indirectly regarded as causing global climatological changes (Zhao et al. 2004). Many other studies in this region of the world have focussed on the relationship between cosmic ray flux and the earth's cloud cover (Carslaw et al. 2002), SSN and precipitation (Zhao et al. 2004), SSN and PWV (Maghrabi & Al Dajani 2014), PWV and temperature (Maghrabi & Al Dajani 2014; Sharifi et al. 2015), PWV and TEC (Suparta et al. 2008; Suparta and Fraser 2014), PWV and solar radiation intensity (Chen and Li 2013). Different studies have reached different conclusions on the strength of the relationship linking the different solar activity and weather parameters (climate indicators), though the results were inconclusive in most cases. Thus, the impact of solar activity on atmosphere dynamics and the physical mechanisms of the relations are still subject to further enquiry. In our contribution to the understanding of the effect that the variability of solar activity has on weather parameters, we explore the relationship between variation of GNSS PWV and four solar activity indicators (namely temperature, SSN, TEC and total solar radiation intensity (TSR)) over Nigeria.

Figures 12, 13, 14, and 15 illustrate the monthly variations of GNSS PWV with temperature, SSN, TSR, and TEC for the study period. In Figure 12, PWV increases with a decrease in temperature. The

months of JJA register the minimum and maximum value for temperature and GNSS-PWV at all the stations from the south to the north of Nigeria. A reverse trend is seen in the months of MAM, when the temperature is at its maximum. The variation in the temperature between the coolest and hottest month is higher at ABUZ and BKFP, which are in the north of the country. A similar variation is seen in PWV estimates at these stations. The interplay between temperature and GNSS- PWV values is best explained by the movement of the tropical air masses. In the north during the months of DJF and MAM, the tropical continental air mass (or Sahara trade wind) from the Sahara tends to increase the temperature and lower humidity, which results in a corresponding decrease in PWV values. In the south, the air mass from the Atlantic Ocean (tropical maritime air mass) is responsible for high humidity and lower temperature in the south and correspondingly increases PWV. The ocean air masses overrun the southern part of Nigeria from February and spread northwards during JJA. The movement of the tropical air masses forces the continental air mass to retreat northward as a result of the sun's movement from the southern to the northern hemisphere (i.e. from the tropic of Capricorn to the tropic of Cancer). During the northward movement of the sun, it crosses the equator in March and is overhead throughout West Africa and thus responsible for the very high radiation and temperature recorded in the months of MAM. The SSNs, as presented in Figure 13, are disturbances (or spots) on the sun's surface that are characterised by severe magnetic activity (i.e. solar flares and hot gassy ejections from the sun's corona). The number of sunspots observable from the earth varies from daily to millennia cycles; the 11-year sunspot cycle remains the most eminent and well probed of these cycles. Over the past century, we have witnessed a warmer earth, at a time when the number of sunspots has also continually been rising. Thus, we may want to attribute the warming of the earth to the influence of solar activity on the global climate. Several climate scientists are of the opinion that sunspots could be playing a part in climate change (e.g. Friis-Christensen and Lassen 1991), while other assess it as quite negligible and ascribe the earths' warming principally to emissions from industrial activity. Figure 13 show that monthly SSN over the period display a similar pattern to the different GNSS-PWV values at all the stations. The sunspots are directly correlated with temperature on the earth and thus as the provider of nearly all the energy in the earths' climate, the sun has a formidable impact on climate.

The TSR amount as depicted in Figure 14 is obviously in an inverse relation with the GNSS-PWV trend at all the locations under investigation. The sun's principal impact on the earth's surface temperature is via inbound TSR. The global temperature change is as a result of energy imbalance attributed to variation in TSR through radiative forcing. TSR and SSN correlate strongly with the solar magnetic field (Wang et al. 2005). The relationship between the sun and the weather is further compounded by the variation in inbound radiation from the sun, which is a result of the balance between declines associated with sunspots and enhancements by faculae (dazzling areas), which surround sunspots. The probe of clouds, where they take place, and their features in relation to TSR play a crucial role in the comprehension of climate change (see Meehl et al. 2003). Low, dense clouds are a sign of solar radiation and cool the surface of the earth. High, weak clouds largely convey inward-bound solar radiation. Simultaneously, they ensnare some of the outward-bound infrared radiation released by the earth and release it back downward, thus heating up the surface of the earth.

The results of the correlation between cloud amount, as shown in Figure 9, and TSR values (Figure 14) confirms the proposition of Meehl et al. (2003): an inverse relation is recorded between cloud amount and TSR at all the stations, with the R^2 values for ABUZ, BKFP and CLBR at 0.7639, 0.5528, and 0.9765, respectively. By comparing the TSR variability between seasons (Figure 14), it is seen that the months of JJA had the lowest record of TSR with a value of 4.56 and 5.24 $kWh/m^2/day$ at ABUZ and BKFP in the north, respectively. Also, in the south of Nigeria lower TSR values of 1.83 and 2.94 $kWh/m^2/day$ were obtained for JJA at CLBR and UNEC, respectively.

In the months of DJF the value of TSR stood at its maximum with an increasing trend northwards. This further reflects the inverse relationship between TSR and GNSS PWV, and their dependence on latitudinal variation. GNSS PWV variation in Nigeria is evidently controlled by the surface radiation balance. This means that a more active season would result from more energy transferring from the related sun activities to the earth's surface through its atmospheric dynamics.
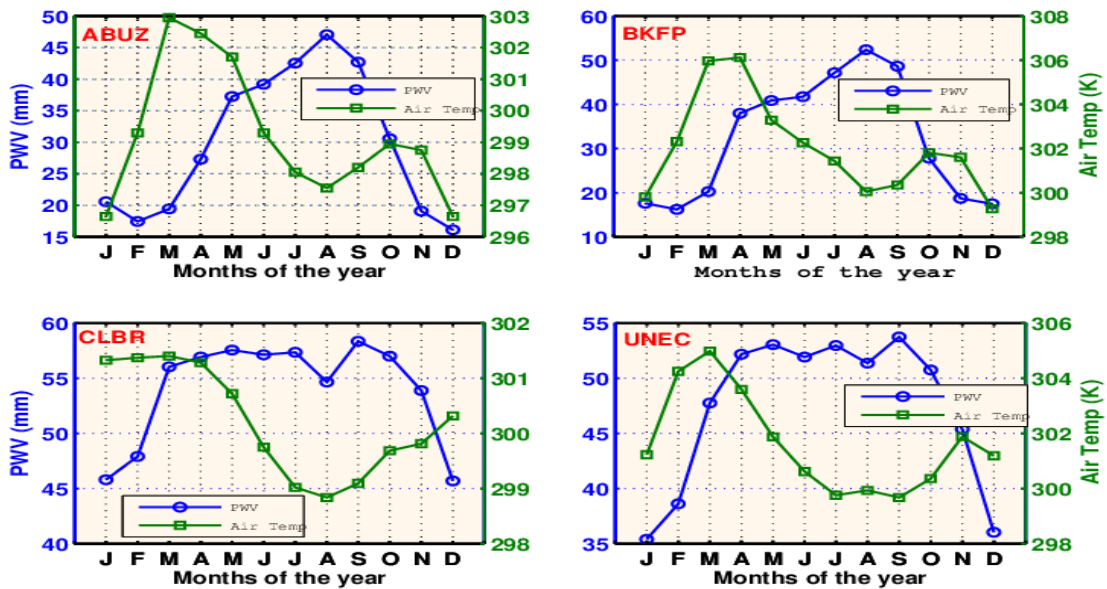

Figure 12: Monthly distribution of PWV (in blue) and temperature (in green) at four GNSS stations (ABUZ, BKFP, CLBR, and UNEC) in Nigeria
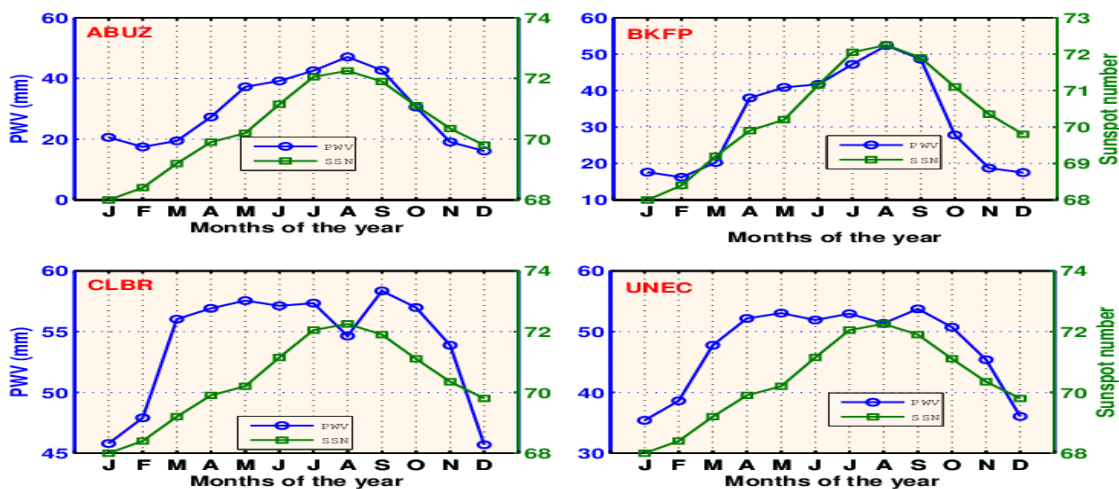

Figure 13: Monthly distribution of PWV (in blue) and SSN (in green) at four GNSS stations (ABUZ, BKFP, CLBR, and UNEC) in Nigeria
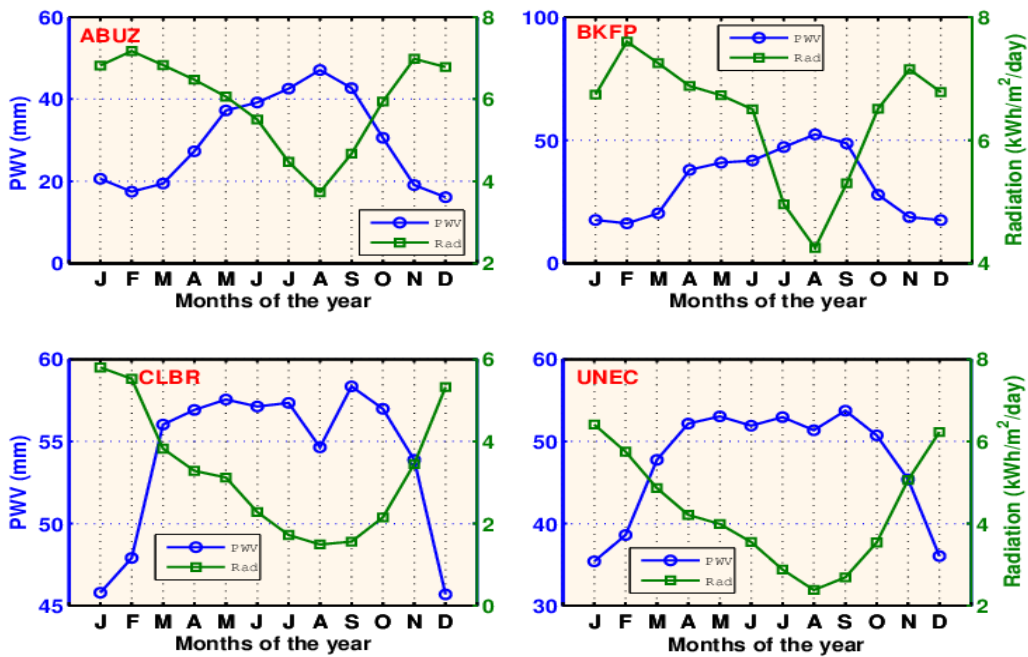
Figure 14: Monthly distribution of PWV (in blue) and total solar radiation intensity (in green) at four GNSS stations (ABUZ, BKFP, CLBR, and UNEC) in Nigeria
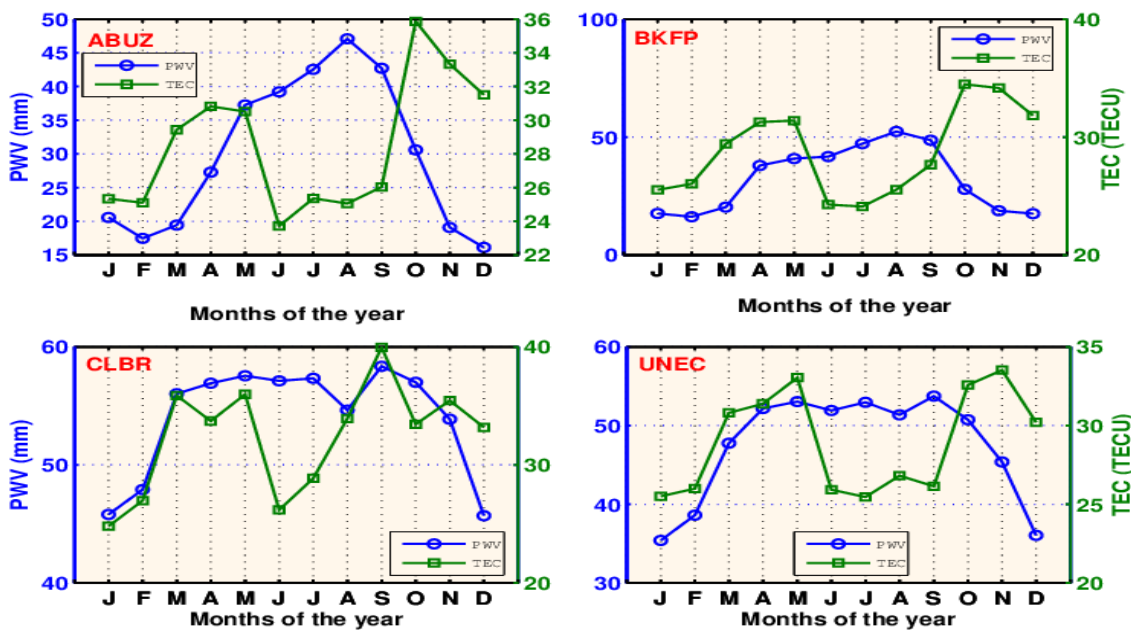
Figure 15: Monthly distribution of PWV (in blue) and TEC (in green) at four GNSS stations (ABUZ, BKFP, CLBR, and UNEC) in Nigeria

The TEC amount shown in Figure 15 is a key ionospheric parameter in monitoring ionospheric conditions and has features that are considerably influenced by the sun. TEC was generated alongside ZTD during the processing of GNSS observation files as described in section 2 of this report; the variation in ZTD is principally controlled by equivalent variations in PWV. The dynamics between the ionosphere and the lower atmosphere remains inadequately elucidated; a clear relationship between PWV and TEC can thus elucidate some of the physical processes through which solar

activity affects terrestrial weather. According to Figure 15, average monthly TEC can be seen to exhibit an inverse relationship with PWV at the different stations. It can also be noticed that TEC values do show weak dependence on latitude and exhibit seasonal patterns with the lowest TEC values recorded in the months of JJA, which correspond to the peak PWV values at all the stations. Similarly, higher TEC values are seen in the months of SON, MAM and DJF, which are periods associated with lower PWV values. The variations in the ionosphere can have a regular or irregular pattern, depending on the geomagnetic activity level. Figure 16 shows the regular daily variation of TEC and PWV at four stations. The daily cycle reveals the difference in water vapour and TEC characteristics for 2013. In Figure 16 the seasonal variation pattern can be viewed from the day-to-day variations at the different stations.
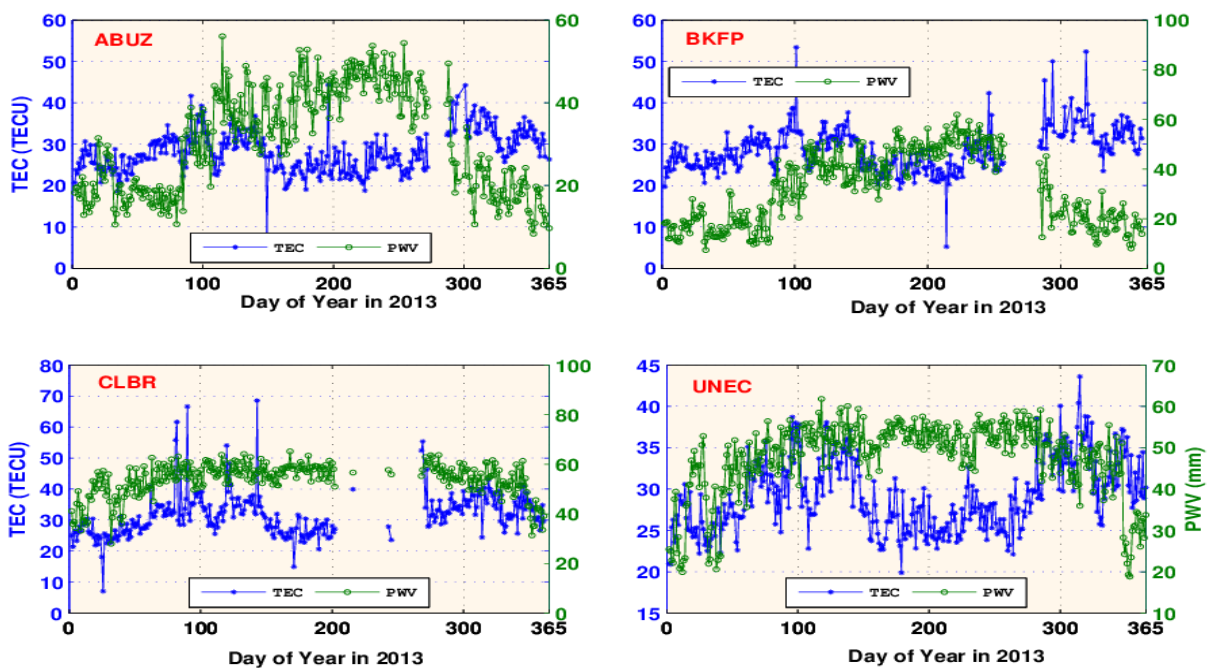

Figure 16: Daily average TEC (in blue) and PWV (in green) variations at four GNSS stations (ABUZ, BKFP, CLBR, and UNEC) for 2013

From the foregoing, it is clear that TEC is temporally and spatially variable. These variations during geomagnetic storms may become rapid and irregular and could cause significant bias in GNSS observation. Therefore, it is interesting to investigate how TEC estimated during an intense geomagnetic activity is linked to the lower atmosphere. This however falls outside the scope of the current study.

In addition, in Figure 16, TEC is seen to exhibit a very conspicuous diurnal and semi-diurnal pattern (in contrast to PWV) with quite similar oscillatory patterns at the different stations; the semi-diurnal cycle for TEC reaches it maximum roughly around two hours after noon, and its minimum is reached before dawn.

The interplay among the different solar attributes as worked out from Pearson's correlation coefficient test is presented in Table 3. GNSS PWV is seen to have a strong positive correlation

(significant at the 0.01 level) with SSN at the different stations. A strong negative correlation (significant at the 0.01 level) is also seen between GNSS PWV and total solar radiation. Interestingly, the correlation between GNSS PWV and the other attributes (temperature and TEC) is weak and insignificant. The SSN and radiation have very strong but negative agreement at all the stations. In addition, there is no statistically significant correlation (insignificant at the 0.01 level) between TEC and the other solar attributes at most of the stations, as shown by entries in red in Table 3.

Table 3: Pearson's correlation coefficient matrix for GNSS- PWV and the different solar events (TEC, radiation, SSN, and temperature) at GNSS locations in Nigeria

Variables	GNSS- PWV	Temp	SSN	TEC	Radiation	GNSS- PWV	Temp	SSN	TEC	Radiation
			ABUZ					BKFP		
GNSS- PWV	1	-0.0820	0.8487	-0.3928	-0.9417	1	-0.0332	0.8315	-0.3780	-0.8199
Temp		1	-0.1761	0.2561	0.2738		1	-0.2277	0.2241	0.4424
SSN			1	-0.0672	-0.8819			1	-0.1055	-0.8186
TEC				1	0.4181				1	0.4415
Radiation					1					1
			CLBR					UNEC		
GNSS- PWV	1	-0.4373	0.6877	0.4881	-0.8735	1	-0.2938	0.7655	0.1291	-0.9103
Temp		1	-0.9311	-0.2513	0.7955		1	-0.7260	0.3138	0.5438
SSN			1	0.3860	-0.9380			1	-0.0950	-0.9114
TEC				1	-0.4167				1	0.1424
Radiation					1					1

The R^2 (coefficient of determination) between GNSS PWV and the different solar attributes is shown in Figure 17. Evidently, this result of the coefficient of determination indicates that the variability in GNSS PWV can be adequately explained or predicted by a similar variation in SSN and TSR at the different GNSS locations under investigation. The predictability of GNSS PWV from TEC observations, as shown in Figure 17, is weak (less than 50%) at all the stations. This is in contrast to previous results from Figure 16, though it may imply that the diurnal relationship between GNSS PWV and TEC is stronger than the seasonal relationship. Notable, also from Figure 17, is the very weak variability accounted for in the monthly GNSS PWV and temperature relationship. This may imply that temperature does not play a major direct role in seasonal water vapour variation in the tropical region of West Africa where this study was conducted. The seasonal variability of water vapour is most probably dominated by that of humidity and the movement of the continental masses. This is contrary to the result of PWV and temperature seasonal relationship reported by some authors in other regions of the world, that suggests that an increase in temperature leads to a corresponding increase in the capacity of water vapour air masses, thus keeping the level away from saturation point and consequently preserving high PWV values (Maghrabi & Al Dajani 2014; Suparta et al. 2008).
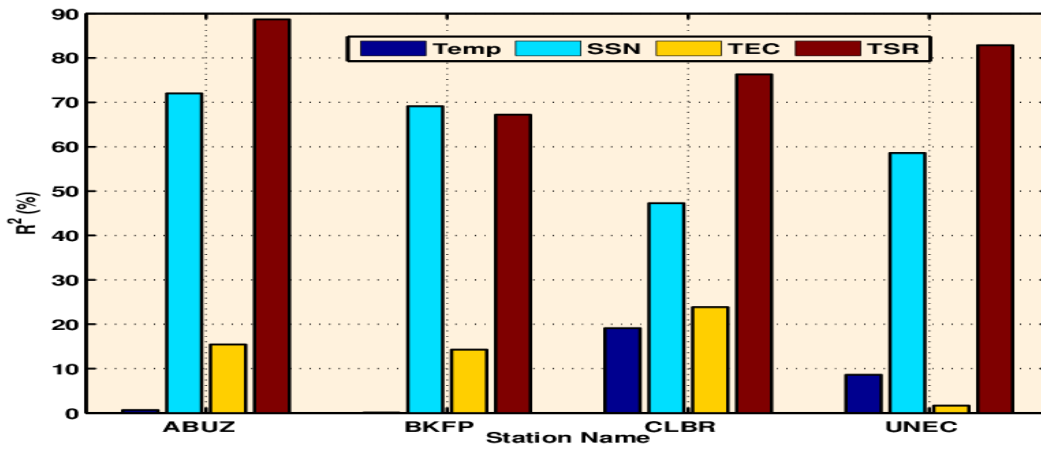
Figure 17: The coefficient of determination (R^2 in %) between GNSS PWV and the different solar attributes at four GNSS stations (ABUZ, BKFP, CLBR, and UNEC) in Nigeria

The relationship as determined from the multivariate analysis between the different solar activity and GNSS PWV at the different regions can be given as follows:

$$
\left.
\begin{aligned}
GNSSPWV_{abuz} &= 302.02 - 1.04*Temp - 1.11*SSN + 0.24*TEC + 8.47*TSR \\
GNSSPWV_{bkfp} &= 888.64 + 2.10*Temp - 4.97*SSN + 0.70*TEC + 6.55*TSR \\
GNSSPWV_{clbr} &= 740.23 - 2.84*Temp + 0.64*SSN - 0.09*TEC + 4.50*TSR \\
GNSSPWV_{unec} &= 29.37 + 0.42*Temp - 1.39*SSN + 0.53*TEC - 6.36*TSR
\end{aligned}
\right\}. \qquad (7)
$$

6. Concluding Remarks

In this paper, PWV was estimated from permanent GNSS stations within the new NIGNET with the objective of assessing the impact and possible applications of the variations in the atmospheric water content as estimated by GNSS. To achieve this objective, GNSS PWV daily estimates were grouped into monthly and seasonal averages; the variations in the monthly and seasonal estimates of GNSS PWV were characterised and correlated with different climate pointers. The climate pointers were broadly classified into rainfall events (rainfall, relative humidity, daylight cloud amount and wind speed) and solar activity (temperature, SSN, TEC, and TSR).

The analysis of the temporal variation of GNSS PWV over Nigeria for the period 2013-2014 revealed that the spatiotemporal changes in PWV content are largely subjugated by the effects of latitude, topographical features, the seasons and the continental air masses. Distinct seasonal cycles were revealed in the GNSS PWV estimates at all the GNSS stations investigated. The marked seasonal cycles are in the wet (rainy) season (during the months of JJA) with maximum PWV and in the dry/Harmattan season (during the months of DJF) with minimum PWV. The variation in PWV content between the period of maximum to minimum occurrence ranges from about 30 mm to 10 mm in the north and south of Nigeria respectively. This is an indication of the high variability in the nature of atmospheric dynamics and climate in the northern part of Nigeria. The study also shows that there is a very strong seasonal interplay among the GNSS PWV, relative humidity, rainfall and cloud estimates. In addition, GNSS PWV and total electron content (TEC) estimates show an opposite relationship; the semi-diurnal relationship between GNSS PWV and TEC is stronger than the seasonal

relationship. The seasonal relation among GNSS PWV, temperature and wind speed appears weak, while very strong interplay exists among the GNSS PWV, sun spot number and total solar radiation estimates.

Undoubtedly, this study has demonstrated the viability of the GNSS meteorology technique over Nigeria as a new observational method with the potential of filling the existing gaps between current observational systems, based on its low cost, continuity, all-weather measuring capability and good spatiotemporal resolution. To explore the Nigerian weather and climate adequately, and to benefit optimally from the GNSS meteorology in Nigeria, further efforts are required. To obtain better correlation between GNSS PWV and meteorological events, it would probably be necessary to introduce the elaboration of slant water vapour contribution along the different lines of sight of GNSS receiver-satellites. If such a GNSS-based PWV measuring system were implemented, near-term/short-range weather forecasting and nowcasting would be possible, which may lead to a reduction in damage due to sudden severe weather conditions. In addition, such data could improve mid-term weather predictability, which is particularly useful for determining the likelihood of the onset of floods or the converse, severe drought. Also, the densification of the NIGNET, which should include the provision of meteorological sensors for PWV retrieval from ZTDs, is suggested. A dense network will contribute valuable water vapour field data for initialisation, setting boundary limits or substantiating NWPs and high-resolution regional climate models.

The results of our study is preliminary in the sense that more complex statistical tests and a longer time period are required to validate the correlation between the different weather events/climate indices that were investigated properly. Long-term climatology would also benefit from the GNSS-derived water vapour time series if this should be made available. However, our results are in good agreement with previous studies around the world (Jin et al. 2008; Suparta 2011) and provide the needed background for further study on the subject of climatic application of GNSS atmospheric products in Nigeria.

7. Acknowledgements

8. References

Adams DK, Fernandes RMS, Kursinski ER, Malia JM, Sapucci LF, Machado LAT, Vitorello I, Monico JFG, Holub KL, Gutman S, Filizola N, Bennett RA (2011) A Dense GNSS Meteorological network for observing deep convection in the Amazon, *Atmos. Sci. Let.*, 12, 207-212. doi: 10.1002/asl.312.

Altamimi Z, Collilieux X, M´etivier L (2011) ITRF2008: An improved solution of the international terrestrial reference frame, *Journal of Geodesy*, 85(8):457–473.

Atedhor GO, Odjugo PAO, Uriri AE (2011) Changing rainfall and anthropogenic –induced flooding: Impacts and adaptation strategies in Benin City, Nigeria, *Journal of Geography and regional planning,* vol.4 (1), pp.42-52.

Benevides P, Catalao J, Miranda, PMA (2015) On the inclusion of GPS precipitable water vapour in the nowcasting of rainfall, *Nat. Hazards Earth Syst. Sci.*, 15:2605–2616. doi:10.5194/nhess-15-2605-2015.

Bevis M, Businger S, Chiswell S, Herring TA, Anthes RA, Rocken C, Ware RH (1994) GPS Meteorology: Mapping Zenith Wet Delays onto Precipitable Water, *J. Appl. Meteorol.*, 33:79–386. doi:10.1175/1520-0450.

Bevis M, Businger S, Herring TA, Rocken C, Anthes RA, Ware RH (1992) GPS meteorology: Remote sensing of atmospheric water vapour using the global positioning system, *J. Geophys. Res*., 97:15787–15801. doi: 10.1029/92JD01517.

Boehm J, Werl B, Schuh H (2006) Troposphere mapping functions for GPS and very long baseline interferometry from European centre for medium-range weather forecasts operational analysis data. *Journal of Geophysical Research B: Solid Earth*, 11(2), Article ID B02406.

Carslaw KS, Harrison RG, Kirkby J (2002) Cosmic rays, clouds, and climate, *Science*, 298(5599), 1732-1737.

Chen J, Li G (2013). Diurnal variations of ground-based GPS-PWV under different solar radiation intensity in the Chengdu plain, *Journal of geodynamics*, 72:81-95. http://dx.doi.org/10.1016/j.jog.2013.08.002.

Cucurull L, Vandenberghe F, Barker D, Vilaclara E (2004) Three-dimensional variational data assimilation of groundbased GPS ZTD and meteorological observations during the 14 December 2001 storm event over the western Mediterranean Sea, *Mon. Weather Rev*., 132:749–763.

Friis Christensen E, Lassen K (1991) Length of the solar cycle: An indicator of solar activity closely associated with climate, *Science*, 254(698700).

Gendt G, Schmid R (2005) Planned Changes to IGS Antenna Calibrations, IGSMAIL #5189, http://igscb.jpl.nasa.gov/mail/igsmail/2005/msg00111.html (accessed 20 December 2015).

Gendt G, Dick G, Reigber C, Tomassini M, Liu Y, Ramatschi M (2004) Near real-time GPS water vapour monitoring for numerical weather prediction in Germany, *Journal of the Meteorological Society of Japan,* 82:361–370.

Guerova G, Bettems J-M, Brockmann E, Matzler C (2006) Assimilation of COST 716 Near-real time GPS data in the non-hydrostatic limited area model used at MeteoSwiss, *Meteorol. Atmos. Phys*., 91:149-164. doi: 10.1007/s00703-005-0110-6.

Gutman S, Sahm R, Benjamin G, Schwartz E, Holub L, Stewart Q, Smith L (2004) Rapid retrieval and assimilation of ground based GPS-Met observations at the NOAA forecast systems laboratory: impact on weather forecasts, *Journal of the Meteorological Society of Japan*, 82:351–360.

Herring TA, King RW, McClusky SC (2006) Reference Manual for the GAMIT/GLOBK GPS software, release, 10.3. Department of Earth, Atmospheric, and Planetary Sciences, Massachusetts Institute of Technology, Boston, USA.

Isioye OA, Combrinck L, Botai JO (2016) Modelling Weighted Mean Temperature in the West African Region: Implications for GNSS Meteorology, *Meteorological Applications*, volume 23, issue 4, 614-632, December 2016. http://dx.doi.org/10.1002/met.1584 .

Isioye OA, Combrinck L, Botai JO (2017) Evaluation of Spatial and Temporal Characteristics of GNSS-derived ZTD Estimates in Nigeria, *Theoretical and applied climatology*, 1-18, 2017, ISSN: 0177-798X. doi: 10.1007/s00704-017-2124-7.

Isioye OA, Combrinck L, Botai JO, Munghemezulu C (2015) The Potential of Observing African Weather with GNSS Remote Sensing, *Advances in Meteorology*, 2015(723071):16. http://dx.doi.org/10/1155/2015/723071.

Jerrett D, Nash J (2001) Potential uses of surface based GPS water vapour measurements for meteorological purposes, *Phys. Chem. Earth (A)*, 26(6-8):457-461. PII: S1464-1895(01)00083-7.

Jin SG, Luo OF (2009) Variability and climatology of PWV from global 13-year GPS observations, *IEEE Trans. Geosci. Remote Sensing*, 47(7):1918-1924. doi: 10.1109/TGRS.2008.2010401.

Jin SG, Li Z, Cho J (2008) Integrated water vapour field and multiscale variations over china from GPS measurements, *Journal of applied meteorology and climatology*, 47:3008-3015. doi:10.1175/2008JAMC1920.1.

Jin SG, Park J, Cho J, Park P (2007) Seasonal variability of GPS-derived Zenith Tropospheric Delay (1994-2006) and climate implications, *J. Geophys. Res.*, 112(D09110). doi: 10.1029/2006JD007772.

Karabatic A, Weber R, Haiden T (2011) Near real time estimation of tropospheric water vapour content from ground based GNSS data and its potential contribution to weather nowcasting in Austria, *Adv Space Res,* 47:1691-1703. doi: 10.1016/j.asr.2010.10.028.

Katsougiannopoulos S, Pikridas C, Zinas N, Chatzinikos M, Bitharis S (2015) Analysis of Precipitable Water Estimates using permanent GPS station data during the Athens heavy rainfall on February 22th 2013. *International Association of Geodesy Symposia*. doi:10.1007/1345_2015_16.

Koizumi K, Sato Y (2004) Impact of GPS and TMI precipitable water data on mesoscale numerical weather prediction model forecasts, *Journal of the Meteorological Society of Japan*, 82(2004):453-457.

Liang H, Cao Y, Wan X, Xu Z, Wang H, Hu H (2015) Meteorological applications of precipitable water vapour measurements retrieved by the national GNSS network of China, *Geodesy and geodynamics,* 2015. http://dx.doi.org/10.1016/j.geog.2015.03.001.

Lu C, Li X, Ge M, Heinkelmann R, Nilsson T, Soja B, Dick G, Schuh H (2015) Estimation and Evaluation of real-time precipitable water vapour from GLONASS and GPS, *GPS solution*. doi: 10.1007/s10291-015-0479-8.

Maghrabi AH, Al Dajani HM (2014) Time Distribution of the precipitable water vapour in central Saudi Arabia and its relationship to solar activity, *Advances in Space Research*, 53:1169-1179. http://dx.doi.org/10.1016/j.asr.2014.02.006.

Mazany A, Businger S, Gutman SI, Roeder W (2002) A lightning prediction index that utilizes GPS integrated precipitable water vapour, *Weather Forecast*, 17(5):1034-1047.

Meehl GA, Washington WM, Wigley TML, Arblaster JM, Dai A (2003) Solar and greenhouse gas forcing and climate response in the twentieth century, *Journal of Climate*, 16(426444).

Musa TA, Amir S, Othman R, Ses S, Omar K, Abdullah K, Samsung L, Rizos C (2011) GPS meteorology in a low latitude region: Remote sensing of atmospheric water vapour over Malaysian Peninsula, *Journal of Atmospheric and Solar Terrestrial Physics*, 73:2410-2422. doi: 10.1016/j.jastp.2011.08.014.

Nilsson T, Elgered G (2008) Long-term trends in the atmospheric water vapour content estimated from ground -based GPS data, *J. Geophys. Res.,* 113(D19101). doi: 10.1029/2008JD010110.

Ning T, Elgered G, Willen U, Johansson JM (2013) Evaluation of the atmospheric water vapour content in a regional climate model using ground-based GPS measurements, *J. Geophys. Res. Atmos.*, 118:329-339. doi: 10.1029/2012JD018053.

Norsuliza Y, Abdullahi M, Ismail M, Zaharim A (2009) A model validation for total electron content (TEC) at an equatorial region. *European Journal of Scientific Research*, 28(4):642-648.

Pikridas C (2014) Monitoring Climate changes on small scale networks using ground based GPS and meteorological data. *Artificial satellites*, 49(3). doi:10.2478/arsa-2014-0010.

Saastamoinen J (1972) Atmospheric correction for troposphere and stratosphere in radio ranging of satellites. In Henriksen, S.W., Mancini, A. & Chovitz, B.H., (Eds.). *The Use of Artificial Satellites for Geodesy*, of *Geophysics Monograph Series*, 15:247–252. Washington, DC: American Geophysical Union (AGU), AIAA, NOAA, U.S.ATC.

Sharifi MA, Khanniani AS, Joghataei M (2015) Comparison of GPS precipitable water vapour and meteorological parameters during rainfalls in Tehran. *Meteorol Atmos Phys,* 127(2015):701-710. doi:10.1007/s00703-015-0383-3.

Song DS, Grejner-Brzezinska, DA (2009) Remote sensing of atmospheric water vapour variation from GPS measurements during a severe weather event, *Earth Planets Space*, 61:1117-1125.

Suparta W (2011) Variability of GPS-Based precipitable water vapour over Antarctica: Comparison between observations and predictions, *World Applied Sciences Journal*, 12(9): 1597-1604.

Suparta W, Fraser GJ (2014) A Case Study of Relationship between GPS PWV and Solar Variability during the Declining Phase of Solar Cycle 23, *Acta Geophysica*, 62(1):220-240. doi: 10.2478/s11600-013-0146-9.

Suparta W, Abdul Rashid ZA, Mohd. Ali MA, Yatim B, Fraser GJ (2008) Observations of Antarctic precipitable water vapour and its response to the solar activity based on GPS sensing, *Journal of Atmospheric and Solar-terrestrial Physics*, 70:1419-1447. doi:10.1016/j.jastp.2008.04.006.

Wang YM, Lean JL, Sheeley NR Jr (2005) Modelling the Sun's magnetic field and irradiance since 1713, *The Astrophysical Journal*, 625(522538).

Zhao J, Han YB, Li ZA (2004) The effect of solar activity on the Annual precipitation in the Beijing area, *Chin. J. Astron. Astrophs.*, 4:189-197.

Zoundi C, Ouattarra F, Fleury R, Amory-Mazaudien C, Duchesne LP (2012) Seasonal TEC variability in West Africa equatorial anomaly region, *Journal of Scientific Research, Euro Journals*, 77(3):309-319, <hal-00968583>.